



HHS Public Access

Author manuscript

ACS Appl Bio Mater. Author manuscript; available in PMC 2021 January 21.

Published in final edited form as:

ACS Appl Bio Mater. 2020 January 21; 3(1): 693–703. doi:10.1021/acsabm.9b01026.

One-Pot Covalent Grafting of Gelatin on Poly(Vinyl Alcohol) Hydrogel to Enhance Endothelialization and Hemocompatibility for Synthetic Vascular Graft Applications

Muhammad Rizwan¹, Yuan Yao¹, Maud B. Gorbet^{2,3}, John Tse¹, Deirdre E. J. Anderson⁴, Monica T. Hinds⁴, Evelyn K. F. Yim^{1,*}

¹Department of Chemical Engineering, University of Waterloo, 200 University Avenue West, Waterloo, ON, Canada N2L 3G1

²Systems Design Engineering, University of Waterloo, 200 University Avenue West, Waterloo, ON, Canada N2L 3G1

³Centre for Bioengineering and Biotechnology, University of Waterloo, 200 University Avenue West, Waterloo, ON, Canada N2L 3G1

⁴Department of Biomedical Engineering, Oregon Health & Science University, Portland, OR 97239, USA

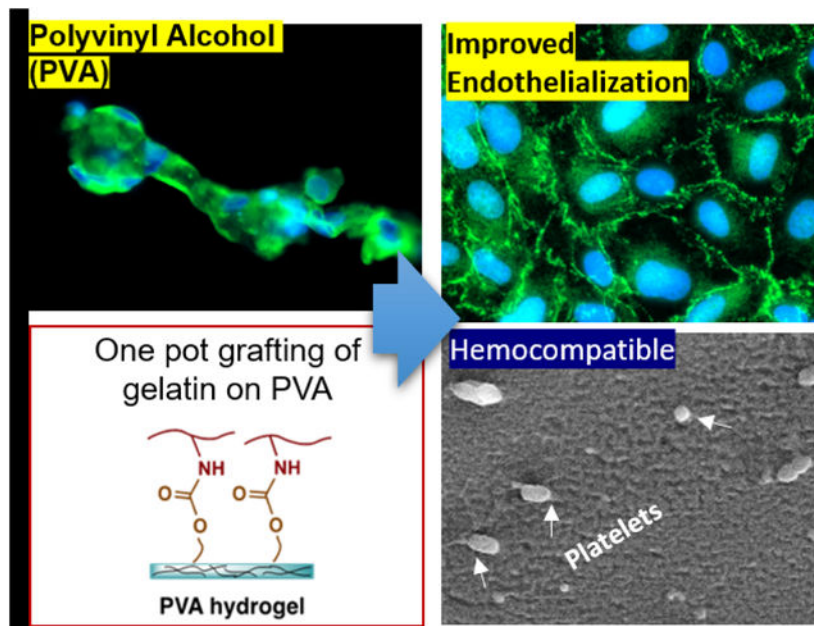
Abstract

Cardiovascular diseases remain the leading cause of death worldwide. Patency rates of clinically-utilized small diameter synthetic vascular grafts such as Dacron® and expanded polytetrafluoroethylene (ePTFE) to treat cardiovascular disease are inadequate due to lack of endothelialization. Sodium trimetaphosphate (STMP) crosslinked PVA could be potentially employed as blood-compatible small diameter vascular graft for the treatment of cardiovascular disease. However, PVA severely lacks cell adhesion properties, and the efforts to endothelialize STMP-PVA have been insufficient to produce a functioning endothelium. To this end, we developed a one-pot method to conjugate cell-adhesive protein via hydroxyl-to-amine coupling using carbonyldiimidazole by targeting residual hydroxyl groups on crosslinked STMP-PVA hydrogel. Primary human umbilical vascular endothelial cells (HUVECs) demonstrated significantly improved cells adhesion, viability and spreading on modified PVA. Cells formed a confluent endothelial monolayer, and expressed vinculin focal adhesions, cell-cell junction protein zonula occludens 1 (ZO1), and vascular endothelial cadherin (VE-Cadherin). Extensive characterization of the blood-compatibility was performed on modified PVA hydrogel by examining platelet activation, platelet microparticle formation, platelet CD61 and CD62P expression, and thrombin generation, which showed that the modified PVA was blood-compatible. Additionally, grafts were tested under whole, flowing blood without any anticoagulants in a non-human primate, arteriovenous shunt model. No differences were seen in platelet or fibrin accumulation between the modified-PVA, unmodified PVA or clinical, ePTFE controls. This study

*Corresponding author: Evelyn K.F. Yim, Department of Chemical Engineering, University of Waterloo, 200 University Avenue West, Waterloo, ON, Canada N2L 3G1 eyim@uwaterloo.ca.

presents a significant step in the modification of PVA for the development of next generation *in situ* endothelialized synthetic vascular grafts.

Graphical Abstract



Keywords

surface modification; anticoagulation; thrombogenesis; blood clotting; endothelial adhesion; hemocompatibility

1. Introduction

Cardiovascular disease remains the leading cause of death in the western world, causing an increased demand for vascular grafts. Commercially available vascular grafts such as ePTFE and Dacron® demonstrate long-term patency at > 6mm diameter,¹ however, their performance is inadequate when used as small diameter vascular grafts (<6 mm) with patency rates of only 35% (ePTFE) to 46% (Dacron®) after 5 years.² The lack of endothelialization is considered one of the major complications in graft failure along with the mechanical mismatch.³⁻⁵ The blood vessel lumen is normally covered with a vascular endothelial cell monolayer at the interface of blood and tissue that performs a pivotal role in maintaining hemostasis.⁶ Vascular endothelial cells secrete biochemical molecules that suppress the initiation of the coagulation cascade.⁷ For example, they secrete prostacyclin and nitric oxide, which are potent inhibitors of platelet activation.⁸ Endothelial cells express ecto-adenosine diphosphatase that degrades adenosine diphosphate and inhibits platelet aggregation.⁹ Therefore, one of the crucial properties of the biomaterials for next generation off-the-shelf small diameter vascular grafts is the ability to facilitate a complete monolayer of vascular endothelial cells to obtain improved patency rates.¹⁰

Polyvinyl alcohol (PVA) is a synthetic polymer that is being developed for several tissue engineering applications.¹¹ Chaouat *et al.* demonstrated the crosslinking of PVA with a food-grade crosslinker and established its potential for use as a small diameter vascular graft.¹² Since then, extensive research studies from our group and others have reported blood compatibility of STMP-crosslinked PVA vascular grafts.^{13–18} Despite its admirable physical and mechanical properties, PVA is not conducive to cell adhesion and spreading due to its lack of cell adhesive ligands and its hydrophilic nature. Unmodified PVA surfaces showed poor endothelial cell attachment in studies conducted *in vitro*¹⁵ as well as *in vivo*.¹² *In vivo*, the extracellular microenvironment contains several biochemical cues in the form of adhesive proteins (such as collagen and fibronectin) in the extracellular matrix (ECM). Cell adhesion is mediated by integrin receptors, which bind to the tripeptide RGD sequence of adhesion proteins in the ECM.¹⁹ Several methods have been demonstrated in the literature to improve cellular adhesion on PVA hydrogel. For instance, mixing of the cell adhesive proteins in the PVA prior to crosslinking to biomimic the native cellular niche is one strategy, which could improve cellular adhesion significantly.^{15, 17, 18, 20} However, physically mixed proteins are prone to leach out of the matrix slowly in the absence of chemical coupling, which may change the bioactivity, microstructure and mechanical properties of the matrix over time due to gradual change in composition.^{16, 21} Another method to improve cellular adhesion is to provide specific topographical cues that favor cell adhesion. We have previously demonstrated that endothelial cell adhesion and other cellular responses can be improved by incorporating patterned topographical cues on the substrate.^{13, 22–24} Treatment of the PVA by using reactive ion plasma is another approach to improve cellular adhesion. Reactive ion plasma has been shown to modify surface elemental composition and surface energy, which improved cellular adhesion by potentially increasing the adsorption of ECM proteins on the surface that facilitate cell adhesion.^{25, 26}

Covalent conjugation of cell adhesion proteins is another widely used strategy to fabricate bioactive surfaces in tissue engineering. Nuttelman *et al.* covalently linked fibronectin on glutaraldehyde crosslinked PVA and studied fibroblast cell attachment.²⁷ However, the conjugation was cumbersome as it required several steps including a dehydration step, which can change the pore size of the hydrogel. Limited knowledge exists on covalent conjugation of cell adhesion proteins on PVA hydrogels to improve primary vascular endothelial cell adhesion for the fabrication of blood compatible synthetic vascular grafts. Additionally, the effect of covalently conjugated ECM proteins on the blood compatibility of the PVA is largely unstudied. An essential criterion for vascular graft material is its ability to provide a blood-compatible interface. This blood-material interaction could potentially activate blood coagulation pathways by activating platelets, that can lead to the formation of blood clot.²⁸ Therefore, it is crucial to conduct in-depth characterization of the blood-compatibility of a surface engineered vascular graft.

We hypothesized that the residual hydroxyl groups on sodium trimetaphosphate (STMP)-crosslinked PVA hydrogels can be activated with carbonyldiimidazole (CDI) to conjugate cell-adhesive proteins via hydroxyl-to-amine coupling in a sequential one-pot reaction. Gelatin was selected as the protein of choice as it has been studied for PVA vascular grafts¹⁶ due to its cell-adhesive ligands,²⁹ gelatin based hydrogels are widely used in tissue engineering applications^{30–32} and products using gelatin-based biomaterial have received

FDA approval.³¹ We studied primary vascular endothelial cell adhesion and monolayer formation by characterizing focal adhesions and cell-cell junction protein expression. As the intended application for vascular grafts and to characterize the effect of covalently conjugated gelatin biomolecule, extensive blood compatibility analysis of the gelatin-grafted PVA was conducted using human platelet rich plasma (PRP) in multiple *in vitro* assays and whole, flowing, non-anticoagulated blood in a shunt, large animal model.

2. Materials and Methods

Fabrication of PVA hydrogels

PVA was crosslinked using sodium trimetaphosphate (STMP) and fabricated into hydrogel films and tubes as described previously.¹⁴ Briefly, 10% PVA (Sigma–Aldrich, 85–124 kDa, 87–89% hydrolyzed) solution was mixed with 15% (w/v) STMP (Sigma Aldrich) and 30% (w/v) sodium hydroxide and cast in petri dishes. The solution was dried for 10 days until fully crosslinked. To fabricate PVA tubes, a 4 mm diameter cylindrical mold was dip-coated with a layer of PDMS and air plasma treated four times for a total of 40 seconds. The molds were then dipped in crosslinked PVA solution for 12 times and placed in ambient temperature until fully crosslinked. The tubes were then demolded by sequential dipping in 10X phosphate buffered saline (PBS), 1X PBS, and deionized water.

Gelatin grafting on PVA hydrogel and its characterization

PVA films or tubes were dried overnight at 60°C to remove moisture. The samples were then incubated in a 100 mg/ml carbonyldiimidazole (CDI) solution in dimethyl sulfoxide (DMSO) for one hour at room temperature with shaking (100 RPM). Subsequently, the samples were washed three times with DMSO and incubated in the gelatin type B (Sigma–Aldrich) solution in PBS (10 mg/ml) overnight at 37°C to produce covalently conjugated gelatin on PVA (PVA-CDI_g). As controls, PVA, which was not activated with CDI, was incubated in gelatin type B overnight (PVA_g) and PVA with activated CDI alone (PVA-CDI) were used. The samples were then washed 3 times with PBS. To characterize the gelatin conjugation, the samples were analyzed using Fourier-transform infrared spectroscopy (FTIR) spectrometer (Shimadzu Scientific) with spectral data spacing of 6 cm⁻¹ for the detection of gelatin specific peaks (Amide I, Amide II).³⁰ Additionally, X-ray photoelectron spectroscopy (XPS) was used to study surface elemental composition. XPS measurements were performed by Thermo-VG Scientific ESCALab 250 Microprobe equipped with a monochromatic Al K α X-ray source (1486.6 eV).

Mechanical properties

Burst pressure was measured by exposing the tubular grafts to increasing intramural pressure until failure. A 4 cm segment of the graft (4 mm diameter) was cut and clamped at one end. The other end was linked to nitrogen gas cylinder through a catheter, and a pressure regulator was used to control the pressure supply.

Uniaxial tensile tests were measured using a Universal Mechanical Tester (UNMT-2MT, T1377, Center for Tribology, Inc.) with a load cell of 100 kg and an extension rate of 10 mm/min. A 6 cm segment of graft was dried at 2 ends to enable adequate gripping, and a 2

cm middle section was kept hydrated for testing. The cross-section area of the graft was pictured and measured by ImageJ.

Primary human umbilical vein endothelial cells (HUVEC) culture and seeding on the hydrogels

Human umbilical vein endothelial cells (HUVECs) were obtained from Lonza. The cells were cultured in Endothelial Cell Growth Medium (EGM-2, Lonza) with 2% fetal bovine serum (FBS) under standard cell culture conditions (37 °C, humidified, 5% CO₂ environment). Cells were passaged at 80–90% confluence by using trypsin (Gibco) and seeded on PVA films for experiments. Prior to seeding, the PVA films were sterilized by ultraviolet light for 30 min. HUVECs were used at passage number 4–5 for all experiments. To investigate cell viability, cell spreading and cell morphology, cells were seeded at a density of 20,000 cells/cm² onto PVA, PVA_g, PVA-CDI_g and glass. Cell viability was analyzed by using Live/Dead assay (Life technologies) at 24 hrs. The samples were incubated for 45 min with calcein AM (3.3 mM) and ethidium homodimer-1 (1.7 mM) (Life Technologies) followed by imaging with fluorescence microscopy (ZEISS Axio Observer). For cell adhesion studies, 24hr after seeding, cells were fixed using 4% paraformaldehyde (PFA) for 20 min. Subsequently, staining was performed for the detection of actin and nuclei using Alexa Fluor™ 488 phalloidin (Life Technologies, 1:500 dilution) and 2 ng ml⁻¹ of 4',6-diamidino-2-phenylindole (DAPI, Sigma-Aldrich) for 30 min at room temperature. The cell attachment was analyzed by counting DAPI stained nuclei. Three images from each sample were analyzed and the experiments were run with triplicate samples. For cell area analysis, the F-actin stained images were analyzed in ImageJ. The cell boundary was manually outlined, and the area was analyzed by using the ImageJ “analyze particle” function.

Formation and characterization of HUVEC monolayer on hydrogels

For the HUVEC monolayer formation assay, glass, PVA, PVA_g and PVA-CDI_g samples were prepared as described earlier and seeded at a higher seeding density of 50,000 cells/cm² to facilitate faster formation of the monolayer. The cells were cultured for 7 days in EGM-2 media and fixed with 4% PFA, washed 1x with PBS and blocked with 10% goat serum and 1% bovine serum albumin (BSA). Following blocking, primary and secondary antibodies were used: (i) Monoclonal mouse anti - zonula occludens 1 (ZO1, 1:50 dilution, BD Biosciences) for 1 hr at room temperature followed by incubation in 2.67 µg/ml of Alexa Fluor 488-conjugated goat anti-mouse antibody (Invitrogen), (ii) Polyclonal rabbit anti VE-cadherin (VE-Cad, 1:200 dilution, Cell Signaling Technology) followed by incubation in 2.67 µg/ml of Alexa Fluor 546®-conjugated goat anti-rabbit antibody (Invitrogen), (iii) Monoclonal mouse anti-vinculin (1:400 dilution; Sigma-Aldrich) followed by incubation in 2.67 µg ml⁻¹ of Alexa Fluor 488®- conjugated goat anti-mouse antibody (Invitrogen). The cells were counterstained to label nuclei using DAPI. To analyze focal adhesions, vinculin stained images were enhanced using the CLAHE algorithm in MATLAB as previously described.²² Subsequently, the images were analyzed in ImageJ by using analyze particle function to determine the size and density of focal adhesions.

Characterization of platelet adhesion with SEM and LDH assay

Blood samples were collected from healthy human donors, who had not taken any medication in the past 48 hours, in polypropylene tubes and anticoagulated with 3.8% sodium citrate (1 ml per 9 ml blood). This study was conducted in accordance with the tenets of the Declaration of Helsinki and received ethics clearance from the University of Waterloo Human Research Ethics Committee. Blood was centrifuged at 200 g for 15 mins at 22°C to prepare platelet rich plasma (PRP). An *in vitro* hemocompatibility assay was performed by incubating PVA and PVA-CDI_g films with PRP (200 µL). Glass coverslips, which had been incubated overnight with 200 µL of 0.1 mg/ml bovine collagen I (Gibco) were used as platelet activating control while commercially available expanded polytetrafluoroethylene ePTFE (W. L. Gore) was used as a negative control. PRP (200 µL) was then added to each sample held down in a 24-well plate with silastic tubing (Dow Corning; Medical grade). Samples were incubated on an orbital shaker for 1 h at 37 °C. After incubation with the samples, PRP was subsequently collected for flow cytometry analysis and real-time thrombin generation assay (TGA), while PVA films were immediately washed in 500 µL ice cold PBS to remove loosely attached platelets. The PVA films were then used for either scanning electron microscopy (SEM) analysis or lactate dehydrogenase (LDH) assay.

Adhered platelets on PVA films were fixed with 2.5% glutaraldehyde in PBS for 20 min. The films were then dehydrated using an ethanol concentration gradient (10%, 30%, 50%, 70%, 90%, 100%). Subsequently the films were incubated in 100% ethanol three times for 5 min each and left to dry at room temperature. Samples were coated with 15 nm gold coating by using metal sputtering system (Denton Desk II). The platelets were imaged in high vacuum mode at 7–10 KeV by using a field emission scanning electron microscope (Zeiss Leo 1550).

The lactate dehydrogenase (LDH) assay was used to quantify the adherent platelets on all the samples. Adherent platelets were lysed by incubating with 1% Triton X-100 at 37 °C for 1 hr. The lysate was stored in –80°C until analysis with LDH assay kit (Roche) per the kit protocol. Absorbance of LDH was correlated to the number of platelets adhered to the PVA samples.¹⁴

For flow cytometry, 5 µL PRP from each sample was diluted in 50 µL DMEM (Gibco) containing 2% FBS. Resting platelets and Phorbol-myristate-acetate (PMA; Sigma-Aldrich) activated platelets were used as controls.³³ PMA was diluted with PBS (1:10; final concentration 2 µM), then added into PRP (10 µL into 50 µL PRP) followed by incubation at 37°C for 10 min to activate platelets. Flow cytometry samples were incubated with fluorescein isothiocyanate (FITC)-conjugated anti-CD61 (BD biosciences) and R-phycoerythrin (PE)-conjugated anti-CD62P (AbD Serotec) for 20 min. At the end of the incubation, samples were diluted and fixed with paraformaldehyde (1% final concentration). All samples were analyzed on the flow cytometer within 5 days. All data were acquired on a Becton Dickinson FACSCalibur flow cytometer (Mountain View, CA, USA) using CELLQuest Software (Mountain View, CA, USA). At least 10,000 platelet events were acquired. Data analysis was performed using FlowJo post data acquisition.

Real time thrombin generation assay

Real time thrombin generation analysis was done with Technothrombin® Thrombin Generation Assay (TGA) kit (Diapharma) according to the manufacturer protocol. In brief, after 1-hour incubation, 40 μ L PRP was collected from the samples and added into a 96-well plate. 50 μ L of the substrate solution was added into each well to initiate the thrombin generation. The supernatant fluorescence (ex: 360 nm, em: 460 nm) was measured by a UV-Vis spectrophotometer (Shimadzu) every minute for 2 hours at 37 °C. The starting time of the thrombin generation (Lagtime), peak thrombin generation, and total amount of thrombin generated were obtained from the thrombin generation curves by using the manufacturer-provided software. The thrombin generation assay was also run in the presence of an external activator, supplied with the kit (RCH activator) that consisted of tissue factor and lipids. For this type of assay, 10 μ L of RCH was added to 40 μ L of PRP followed by the addition of the substrate. The fluorescence readings and data analysis were performed as described above.

Ex vivo shunt testing

PVA-CDIg and plain PVA tubes were tested in a non-human primate, *ex vivo* shunt model to determine platelet and fibrin accumulation in whole blood in the absence of anticoagulants, as described previously.¹ In short, PVA tubes were connected to silicone tubing in a chronic, arteriovenous femoral shunt. Platelet accumulation on each surface was quantified every minute for 1 hr from the radiation of autologous, In¹¹¹-labeled platelets. Fibrin accumulation was measured as an endpoint value from homologous, I¹²⁵-labeled fibrinogen after the In¹¹¹ decayed. Clinical, 4mm inner diameter, ePTFE grafts (W. L. Gore) were also tested as clinical controls (n=2–6 per group). Collagen I-coated ePTFE grafts were tested to confirm animal reactivity to a positive control and were not included in the analyses.

Shunt data were collected from 2 juvenile, male baboons (*papio anubus*) who were cared for at Oregon National Primate Research Center (ONPRC) following the “Guide to the Care and Use of Laboratory Animals” prepared by the Committee on Care & Use of Laboratory Animals of the Institute of Laboratory Animal Resources, National Research Council (International Standard Book, Number 0-309-05377-3, 1996). Animal studies were approved by the ONPRC Institutional Animal Care and Use Committee.

Statistical analysis

All data are presented as mean \pm Standard Deviation (SD). To determine the statistical significance of multiple comparisons, one-way ANOVA with Tukey’s *post hoc* test was used in GraphPad Prism. For the *ex vivo* shunt testing, shunt statistics were analyzed using R (R Foundation for Statistical Computing, version 3.5.1). Platelet data were analyzed with a multi-way repeated measures ANOVA using a fractional polynomial term (Time \times Ln(Time)) and interactions. Platelet data were natural-log transformed prior to analysis, to approximate normality and improve fit. In order to avoid the exclusion of zero by the transform, 0.01 was added to each value before the transform. Fibrin data were normalized per unit length of the grafts and analyzed with a one-way ANOVA and Tukey’s *post hoc* test. Collagen ePTFE data were not included in these analyses since only 2 datasets were collected for this group

for the purpose of confirming animal reactivity and is not of interest for the material comparison. The statistical significance threshold was set at $p = 0.05$.

3. Results

3.1. Fabrication and characterization of gelatin grafted PVA hydrogel

Gelatin grafting was achieved by using carbonyldiimidazole (CDI) to link hydroxyl group on PVA hydrogel and amine groups on gelatin, as shown in schematic diagram in Fig 1a. We quantified the success of hydroxyl-to-amine coupling by using FTIR. All of the FTIR spectra (PVA, PVA-CDI, PVAg, PVA-CDI_g) showed similar characteristic PVA peaks such as broad O-H peak ($\sim 3200\text{--}3400\text{ cm}^{-1}$), C-H stretching ($\sim 2936\text{ cm}^{-1}$), C-O peak ($\sim 1142\text{ cm}^{-1}$) and C-O-C peak ($\sim 1091\text{ cm}^{-1}$). However, differences were noted in $1500\text{--}1700\text{ cm}^{-1}$ region of the FTIR spectra. In the FTIR spectrum, gelatin can be identified by Amide I peak between $1600\text{--}1700\text{ cm}^{-1}$ mainly due to the C=O bond stretching vibration and Amide II peak between $1500\text{--}1600\text{ cm}^{-1}$ mainly due to the N-H bond stretching vibration. The FTIR data showed the presence of both of these peaks (Amide I at $\sim 1656\text{ cm}^{-1}$ and Amide II at $\sim 1548\text{ cm}^{-1}$) in covalently-grafted gelatin PVA (PVA-CDI_g), which indicated the conjugation of gelation molecules on the PVA surface (Fig 1b). PVA alone, PVA activated in CDI but not incubated in gelatin (PVA-CDI) and PVA incubated in gelatin (PVAg) did not show Amide II peak (Fig 1b). However, a small peak was present at $\sim 1654\text{ cm}^{-1}$, which could be due to C=O from the acetate groups in PVA backbone.

Gelatin biomolecules also contain nitrogen (N), which could further differentiate it from the PVA. An XPS survey scan was performed on PVA, PVA-CDI, PVAg and PVA-CDI_g to analyze the surface. Only the PVA-CDI_g showed a strong N1s peak (Fig 1c). Conversely, PVA-CDI and PVAg showed weak N1s peak. Atomic percentage analysis from the XPS survey scan showed that PVA-CDI_g had $8.9\pm 1.1\%$ nitrogen compared to $0.7\pm 0.8\%$ in PVAg and $0.3\pm 0.2\%$ in PVA-CDI (Fig 1c). The small nitrogen signal in PVA-CDI could result from imidazole carbamate, which is an intermediate active group.³⁴ PVAg also showed only a small amount of nitrogen, which showed that much of the gelatin was washed away during washing steps and did not remain on the PVA surface. In PVA alone, the nitrogen could not be determined. Taken together, FTIR and XPS data showed that the gelatin was successfully grafted on the surface of PVA hydrogel using the CDI one-pot technique.

Previous studies have shown that the mechanical properties of the STMP-crosslinked PVA vascular grafts closely match the blood vessels. To understand the effect of the gelatin conjugation on the mechanical properties of the PVA, we characterized the tensile Young's modulus and burst pressure of the modified PVA. The results showed that the tensile modulus as well as burst pressure of the PVA-CDI_g were similar to PVAg and PVA (Fig 2a,b). This showed that the CDI based gelatin conjugation on PVA did not significantly alter the mechanical properties of the STMP-crosslinked PVA.

3.2. Covalently-conjugated gelatin on PVA hydrogel improved primary HUVECs adhesion, spreading, and viability

The effect of gelatin conjugation to PVA on HUVEC adhesion was studied using films of PVA-CDI_g with controls of unmodified PVA, PVAg and glass. The phase contrast images at 4 hrs after seeding demonstrated cell attachment and spreading on PVA-CDI_g and glass, while minimal cell attachment and no cell spreading was observed on unmodified PVA or PVAg (Fig 3a). HUVECs viability was characterized at 24 hrs after seeding with a Live/Dead assay (Fig 3b), which showed high cell viability on PVA-CDI_g similar to glass control, validating that the cells not only attached to the PVA-CDI_g, but also remained viable. Conversely, at 24 hrs almost no cells were observed on PVA or PVAg. Live/dead assay results showed that the side products of the CDI reactions were washed away during sample washing and did not cause cytotoxicity for cells.

The cell density and spreading were quantified by using phalloidin staining 24 hrs after seeding (Fig 3c). A significantly higher number of HUVECs were found on the PVA-CDI_g ($16.0 \times 10^3 \pm 5.2 \times 10^3$ cells/cm²; $P < 0.0001$) or PVAg (1545 ± 522 cells/cm²; $P < 0.0001$), which correlated to the live/dead assay in terms of cell attachment on the different groups (Fig 3d). The number of cells on the PVA-CDI_g was lower than on the glass ($25.7 \times 10^3 \pm 3.4 \times 10^3$ cells/cm²; $P < 0.05$). Cell spreading is another important parameter in cell-matrix interaction that indicates the strength of adhesion on substrates. Cell spreading on PVA-CDI_g (2023 ± 312 μm²) was comparable to that of the glass (2142 ± 130 μm²). The cellular spreading was significantly lower on PVA (424 ± 270 μm²; $P < 0.001$) and PVAg (913 ± 109 μm²; $P < 0.01$) compared to PVA-CDI_g. These results showed that the surface of the gelatin-grafted PVA was indeed more conducive to cellular adhesion, specifically improving cell adhesion and spreading. This also revealed that the mere incubation of the PVA in gelatin solution did not improve cellular functions, due to a lack of adsorption on the surface of PVA.

3.3. HUVECs formed a complete monolayer and expressed functional markers on gelatin-grafted PVA

As the lumen of the blood vessel is lined with the endothelial monolayer *in vivo*, we analyzed whether the PVA-CDI_g could support the formation of the HUVECs monolayer, which expresses focal adhesions and cell-cell junction protein markers. After 7 days of seeding, a monolayer was seen on both glass control and PVA-CDI_g, but cells failed to form a monolayer on the PVA and PVAg (Fig 4a). A few clumps of cells were observed on PVA or PVAg while most of the surface was not covered by any cells. Focal adhesions (FAs), which indicate a stable and strong cell-matrix adhesion, were analyzed in the monolayer via vinculin staining, a protein which is a component of the focal adhesion complex. HUVECs on PVA-CDI_g and on the glass control demonstrated characteristic punctate FAs of an endothelial monolayer (Fig 4a). Quantitative analysis of the focal adhesions showed that the FA size and density were similar on glass and PVA-CDI_g surface (Figure 4a). FAs were not detected on the cell clump on PVA and PVAg.

We further analyzed the expression of ZO1 and VE-Cad, which are expressed at cell-cell junctions if the endothelial cells form a tightly knit monolayer (Fig 4b-c). On PVA-CDI_g,

similar to observations on glass, both ZO1 and VE-Cad proteins were expressed strongly at the cell periphery instead of the cytoplasm. PVA and PVAg were omitted from the cell-cell junctional protein analysis due to cell's inability to form a monolayer. The data on the HUVEC studies showed that gelatin conjugation by CDI on the PVA hydrogel generates a surface, which is conducive for endothelial cell adhesion, spreading, and ultimately monolayer formation.

3.4. Effect of gelatin grafting on platelet activation

Platelet activation and subsequent platelet-platelet adhesion is a critical indicator of thrombosis. To investigate the effect of gelatin conjugation on the blood compatibility of the PVA, we studied platelet adhesion by SEM and an LDH assay. SEM images showed that the platelet adhesion on PVA-CDIg was similar to ePTFE and PVA (Fig 5a). Very high platelet attachment and deposition were observed on collagen-coated glass (glass) that was used as a positive control (Fig 5a). To quantitatively verify the platelet adhesion on different samples, a lactate dehydrogenase (LDH) assay was performed, which measures the amount of LDH released from the platelets attached to the surface, and thus can be used as an indicator of relative platelet adhesion. PVA and PVA-CDIg had significantly lower absorbance compared to the glass ($p < 0.05$ for both) (Fig 5b); however, the platelet adhesion on PVA or PVA-CDIg was comparable, showing that gelatin conjugation did not alter the blood platelet adhesion level. The LDH assay absorbance for the ePTFE control was also similar to that of PVA-CDIg (Fig 5b). Overall, the LDH assay complemented the SEM results regarding platelet attachment.

Platelet activation was further analyzed by flow cytometry to assess microparticle generation and expression of CD61 and CD62P, which are upregulated on activated platelets.³⁵ The platelets were identified as CD61+ events in scatter plots, which are shown in supplementary Fig S1. As expected, the expression of CD61 (also known as integrin $\beta 3$ or glycoprotein IIIa) as well as CD62P (P-selectin) were significantly higher on the PMA-activated platelets (positive control) compared to platelets in all other groups including glass, confirming that the PMA acts as a strong platelet activator (Fig 5c–d). CD61 and CD62P expression was similar on PVA, PVA-CDIg, and ePTFE. The expression of CD61 and CD62P on resting platelets were also similar to all of the tested groups, which indicated that there was no significant material-induced upregulation in platelet activation compared to resting control. Platelets also produce microparticles which are shed due to loss of cytoskeleton-membrane adhesion upon platelet activation and interactions with a biomaterial.³⁶ Platelets on PVA-CDIg produced almost 60% less microparticles compared to resting control and almost 66% less microparticles compared to PVA (Fig 5e); however, the results were not statistically significant. Microparticles formation following interactions with PVA-CDIg was comparable to that of ePTFE. Overall, the flow cytometry analysis suggests that the gelatin conjugation neither negatively impacted nor significantly improved the blood compatibility of PVA.

3.5. Realtime thrombin generation analysis

Thrombin enzyme mediates the cleavage of fibrinogen to fibrin, which ultimately leads to thrombus (blood clot) formation.³⁷ Thrombus formation is a major complication for blood contacting materials. Therefore, we assessed real time thrombin formation kinetics due to

the activation of material-induced intrinsic pathway by using thrombin-specific fluorogenic substrate. Typical kinetic curves of the thrombin generation are presented in Fig S2. Various parameters were deduced and analyzed from the thrombin formation kinetic curve (Fig 6). Lag-time (time required for thrombin generation to begin) was shortest on glass (13.1 ± 6.8 min), due to presence of collagen, which is known to favor the formation of thrombus.³⁸ The lagtime on PVA-CDIg (50.1 ± 19.8 min) was longer than the PVA (27.9 ± 9.0 min) and ePTFE (37.8 ± 13.5 min); however it was not statistically significant (Fig 6a). This showed that initiation of coagulation is delayed on PVA-CDIg. We further looked at the peak thrombin formation where the following general trend was seen: Glass > PVA > ePTFE > PVA-CDIg (Fig 6b). Peak thrombin formation with PVA-CDIg (162.7 ± 65.9 nM) was significantly less compared to PVA (325.3 ± 66.2 nM) ($P < 0.05$) and slightly slower compared to ePTFE (196.3 ± 58.31 nM). Total thrombin generation, which is a balance between the hypo and hypercoagulant components in the plasma, was lower on PVA-CDIg (2326 ± 1432 nM) compared to PVA (4196 ± 729 nM) and slightly less compared to ePTFE (3253 ± 1101 nM) (Fig 6c). As expected, glass had the highest total thrombin generation of all the groups. We also studied the thrombin generation in the presence of extrinsic thrombin pathway activator (supplied with the assay kit). The lag time further decreased and total thrombin increased from all samples; however, the trends did not change (Fig S3). In summary, the thrombin formation assay showed that the gelatin conjugation, which enabled endothelialization, also improved thromboresistance on the PVA surface.

3.6. Ex vivo shunt assay on tubular PVA-CDIg vascular grafts

PVA and PVA-CDIg tubular grafts were tested in a baboon *ex vivo* shunt assay. Platelet data showed no significant differences among PVA-CDIg, PVA, and ePTFE samples (Fig 7a, $p = 0.071$). Nor were significant differences observed between fibrin accumulation in the various groups (Fig 7b, $p = 0.226$), although both PVA and PVA-CDIg trended lower than the ePTFE control group. PVA-CDIg and PVA groups showed nearly identical platelet and fibrin reactivity suggesting that the modifications did not increase coagulation potential *ex vivo*. The lack of change from the clinical control, ePTFE, also supports the thromboresistance seen *in vitro*.

4. Discussion

This study presented a facile one-pot covalent conjugation of a cell-adhesive protein on the PVA to facilitate endothelialization of the surface while retaining blood compatibility. The technique presented here is generic in nature and could be performed on other hydroxyl group containing hydrogels (e.g. freeze thaw PVA hydrogel and hyaluronic acid hydrogels). CDI has been applied to covalently bind proteins on the surfaces of various materials.²⁷ This study, for the first time, showed that CDI generates protein functionalization via covalent grafting on PVA hydrogel. STMP crosslinking of the PVA has been well studied and the mechanisms have been proposed.³⁹ For the CDI-based hydroxylamine reaction, the unreacted OH groups from the STMP-crosslinked PVA were targeted. Hydroxylamine coupling reactions are known to proceed at a pH that is two points above the isoelectric point of the proteins.⁴⁰ Gelatin type B has an isoelectric point of around 5, while the isoelectric point of gelatin type A is between 7 to 9. Therefore, the reaction with gelatin type

A will demand a highly basic environment. However, when gelatin type B is used, hydroxylamine coupling could theoretically be performed in the PBS buffer (pH 7.4). We obtained successful conjugation in PBS with overnight incubation at 37 C as confirmed by FTIR and XPS data. This coupling method was also applied on widely used freeze-thaw PVA hydrogels.⁴¹ Cellular adhesion was observed on freeze-thaw PVA hydrogels after the CDI based gelatin conjugation (Fig S4). This shows that the CDI based hydroxylamine conjugation of proteins could be performed in conjunction with other PVA crosslinking methods as long as unreacted hydroxyl groups are available for modification.

The high failure rates of clinically-utilized small diameter synthetic vascular grafts such as Dacron® and ePTFE are likely due at least in part to the lack of endothelialization. Recent studies have demonstrated the applicability of PVA as a replacement of current commercial grafts for small diameter vascular grafts applications, including studies conducted in animal models.^{12–16, 42–46} We had previously validated submillimeter PVA graft application for microvascular surgery in a rabbit animal model.⁴² Despite these promising results, the lack of endothelialization remains a bottleneck to further develop PVA as a viable choice for long term success of small diameter vascular grafts.

PVA is inherently hydrophilic which prevents protein adsorption on the surface^{27, 47} and, as previously presented, no cell attachment was observed on PVA after overnight incubation in gelatin. Therefore, an alternative strategy is required to render PVA surface biomimetic and conducive for *in situ* cellular attachment. Physical mixing of cell adhesive proteins in PVA solution prior to PVA crosslinking is one potential method that has been demonstrated to produce significantly improved cell adhesion.^{15, 17} More recently, studies showed that the physically-mixed biomolecules in PVA hydrogels could slowly release from the graft. Close to 50% of the mixed protein leached during a 12-week study.¹⁶ This process also changed the pore size of the graft surface, which could additionally alter the mechanical properties of the materials.¹⁶ The release of proteins from PVA is not surprising as there was no proven covalent bonding mechanism between the biomolecule and the PVA in STMP crosslinking. Previous attempts to crosslink the gelatin alone by using STMP have failed, which revealed that STMP does not activate functional groups in gelatin.¹⁵ In another study, incorporation of the RGD peptide motifs in PVA solution slightly improved the cell viability on PVA hydrogel; however, the combination of the biochemical cues from an RGD peptide and topographical cues on PVA surface acted synergistically to significantly improve the cell viability and adhesion on PVA.¹⁴ Another notable technique to improve the PVA bioactivity is the treatment of PVA with reactive ion plasma, which significantly improved endothelial cell adhesion on PVA.^{25, 26} These studies found that the application of plasma introduced nitrogen on the PVA surface and reduced the surface energy of the PVA, which were thought to improve cell adhesion by increasing surface adsorption of the extracellular matrix proteins. Building on the previous studies, the technique presented in this study demonstrates a facile and highly efficient method to conjugate cell adhesive gelatin protein on PVA hydrogels without interfering in the hydrogel preparation protocol.

The CDI based technique demonstrated here could also be applied to conjugate other proteins with NH₂ reactive groups by adjusting the reaction pH to above the isoelectric point of the protein.

Primary HUVECs displayed significantly improved cellular adhesion, viability and spreading on PVA-CDIg compared to PVA alone. Spreading of the cells is an indication of the strong cell-matrix interaction where higher cell area results in higher adhesion strength.⁴⁸ The expression of focal adhesions (FAs), which serve as anchoring points for the cells, can be used to monitor this cell adhesion.²² Cell spreading also positively, but nonlinearly correlates to the FAs size.⁴⁹ Cells on PVA or PVAg did not express FAs in this study, which could explain the very low cell adhesion on the PVA or PVAg. However, PVA-CDIg demonstrated a high cell density and the adhesion area, which was comparable to the coverslip controls. Stiffness is a well know modulator of cell spreading where a stiff substrate leads to higher cell spreading.^{50, 51} Similarly, surface ligands are also shown to control cell spreading. The glass coverslips were not functionalized with cell-adhesive proteins, and are a stiff substrate. Therefore, cell spreading on the glass was mainly governed by stiffness.^{52, 53} However, cell spreading on PVA, which is a flexible material compared to glass, is mainly due to the presence of cell-adhesive ligands. The cells on PVA-CDIg expressed FAs, which confirmed that the cells were readily able to bind to the RGD sequence of the gelatin molecule and clustering of integrins led to the formation of FAs. The FA expression of the HUVECs on PVA-CDIg was comparable to the glass, which showed strong cell-material interaction. The cells are subject to shear force *in vivo*.⁵⁴ Therefore cell adhesion should be stable under flow. We anticipate that the cells have strong adhesion to the PVA-CDIg to withstand the shear force induced by flow. However future studies should be conducted to subject the adhered cells to shear flow to investigate the stability of the cells under flow.

Mere adhesion and spreading of cells may not necessarily mean a complete monolayer will eventually form. An incomplete monolayer may expose blood platelets to the underlying ECM, which activates platelets.³⁸ One of the hallmarks of tightly-knit and complete monolayer is the expression of tight junction proteins that play an important role in tissue integrity.⁵⁵ Endothelial cells interact with each other and express transmembrane proteins such as ZO1 and VE-Cad to maintain their barrier property, reduced permeability, and an anti-thrombogenic state in the blood vessels.⁵⁶ Therefore, regenerated monolayers on clinically relevant graft materials should be analyzed for the expression of these tight junctional proteins. The *in vitro* regenerated endothelium on PVA-CDIg showed positive expression of ZO1 and VE-Cadherin, demonstrating the formation of the monolayer. This validated PVA-CDIg as a material that promotes complete endothelialization of the surface. Endothelialization performs a pivotal role in maintaining homeostasis by performing functions such as suppressing the initiation of the coagulation cascade and inhibition of platelet activation and platelet aggregation.⁷⁻⁹ Inhomogeneous distribution of the gelatin is a concern which could lead to patchy cell attachment and incomplete monolayer formation. To verify that the gelatin is uniformly distributed, we imaged HUVEC monolayer at low magnification and used uniform cellular adhesion as a proxy for the distribution of gelatin on the surface. The fluorescence images taken at different random regions of the samples showed that the samples were fully covered with monolayer without any patches and cell free areas (Fig S5). This demonstrated that the gelatin was uniformly distributed over the surface to allow for homogenous cellular attachment.

While a monolayer is desired for maintaining vascular homeostasis, the underlying material must be non-thrombogenic. Undoubtedly, blood compatibility is of utmost importance for any materials intended to be used as vascular grafts. Any strategies that improve cellular adhesion but compromise on the blood compatibility of the material would be unsuitable. Therefore, blood compatibility was assessed using multiple *in vitro* assays including platelet adhesion, activation marker expression and thrombin generation and whole blood *ex vivo* testing. It was shown that gelatin conjugation improved the performance of the gelatin-conjugated PVA as compared to the unmodified PVA, which was statically significant in case of peak thrombin formation and considerably better but not statistically significant in other cases (lag time of thrombin formation, *ex vivo* shunt assay, total thrombin formation, microparticle generation, and fibrin accumulation). Of the different assays for blood compatibility testing, the *ex vivo* shunt study is a robust model that uses whole blood under arterial flow rates without the addition of anticoagulant to characterize material blood compatibility. Additionally, it combines platelet activation and fibrin accumulation examination under hemodynamically relevant conditions, which makes it more likely representation of clinical performance. In this clinically relevant model, the PVA-CDI_g performed equivalently to the current clinical standard of ePTFE.

Gelatin is a denatured form of collagen, and therefore, has the same chemical structure as that of collagen.⁵⁷ Collagen receptors have been identified on platelets⁵⁸ Exposure to collagen is known to induce platelet activation and collagen coated glass is routinely used as positive controls for platelet activation, therefore, such an effect of gelatin on biomaterials hemocompatibility may seem counter-intuitive at first. Multiple studies, however, have reported that the gelatin has either no influence or positive influence on the blood compatibility of the biomaterials.^{4,18, 26, 59} For example, polycaprolactone functionalized with gelatin molecules reduced platelet activation and significantly improved anti-thrombogenic profile of endothelial cells.⁶⁰ Ino *et al.* showed that gelatin mixed in PVA hydrogel reduced the platelet adherence on the surface and increased the lagtime of thrombin generation.¹⁵ Gelatin also improved the patency rate of grafts when gelatin-mixed PVA grafts were studied *in vivo* in a recent study.¹⁶

Several other studies have reported similar results when gelatin incorporated biomaterials were used as blood contacting devices.^{4, 59, 61} Based on the available knowledge, it could be speculated that the platelets respond differently to gelatin and collagen, which could potentially be due to the presence of self-assembled structures in collagen molecules giving rise to the fibrous topography of collagen. Three polypeptide strands of collagen coil with each other to form the triple helix structure. These triple helical structures self-assemble to form higher order collagen fibrils that leads to the formation of collagen fibers.⁶² This self-assembly process eventually give rise to fibrous topography of the collagen, which is lost when collagen is denatured to obtain gelatin. Therefore, it could be speculated the platelets could sense and respond to the fibrous structures of the collagen material, which is not present when the platelets are exposed to gelatin biomolecules. This speculation is supported to some extent by a study by Zhang *et al.* where gelatin functionalized nanofibrous scaffolds clearly showed high platelet adhesion, which demonstrated that the nanofibrous topography could play important role in platelet activation.⁵⁶ In short, the gelatin molecules at the PVA surface did not reduce the blood compatibility of the PVA grafts.

Conclusions

This study detailed a new method of covalent conjugation of proteins on the PVA surface in a simple one-pot reaction where the protein was grafted at physiological temperature and pH. The conjugation strategy developed in this study could also be applied to other types of hydrogels with hydroxyl groups such as hyaluronic acid and polysaccharides-based hydrogels. Gelatin presentation on the PVA surface did not alter the mechanical properties of the PVA. The resulting gelatin-conjugated PVA supported vascular endothelial cell response in terms of adhesion, spreading, and development of a confluent monolayer with strong cell-cell interactions, while demonstrating hemocompatibility comparable to a clinical gold-standard control. Fabrication of such PVA synthetic vascular grafts that facilitate endothelialization without increasing thrombosis could lead to remarkable progress for the development of next generation off-the-shelf small diameter synthetic vascular grafts with high patency rates.

Supplementary Material

Refer to Web version on PubMed Central for supplementary material.

Acknowledgment

We greatly appreciate the contributions of Mr. Matthew Hagen, Ms. Jennifer Johnson, Ms. Tiffany Burch, and the ONPRC (funded by NIH grant award P51OD011092) staff for their help in data collection and analysis of the shunt studies. Financial support for this work was provided by NIH Grants R01HL130274, R01HL144113, and R01DE026170, and the work was partially supported by the National Natural Sciences and Engineering Research Council (NSERC) of Canada Discovery Grant (RGPIN-2016-04043), and the University of Waterloo Startup Fund. Y.Y. received financial support from NSERC CREATE (401207296). J.T. would like to acknowledge financial support from the WIN Fellowship of the University of Waterloo Institute of Nanotechnology.

References

1. Pashneh-Tala S; MacNeil S; Claeysens F, The Tissue-Engineered Vascular Graft-Past, Present, and Future. *Tissue Eng Part B Rev* 2015, 22(1):68–100. [PubMed: 26447530]
2. Devine C; McCollum C; North West Femoro-Popliteal Trial, P., Heparin-bonded Dacron or polytetrafluorethylene for femoropopliteal bypass: five-year results of a prospective randomized multicenter clinical trial. *J. Vasc. Surg* 2004, 40 (5), 924–31. [PubMed: 15557906]
3. Zilla P; Bezuidenhout D; Human P, Prosthetic vascular grafts: Wrong models, wrong questions and no healing. *Biomaterials* 2007, 28 (34), 5009–5027. [PubMed: 17688939]
4. Zhao Q; Cui H; Wang J; Chen H; Wang Y; Zhang L; Du X; Wang M, Regulation Effects of Biomimetic Hybrid Scaffolds on Vascular Endothelium Remodeling. *ACS Applied Materials & Interfaces* 2018, 10 (28), 23583–23594. [PubMed: 29943973]
5. Zhao Q; Wang J; Cui H; Chen H; Wang Y; Du X, Programmed Shape-Morphing Scaffolds Enabling Facile 3D Endothelialization. *Adv. Funct. Mater* 2018, 28 (29), 1801027.
6. van Hinsbergh VWM, Endothelium-role in regulation of coagulation and inflammation. *Semin. Immunopathol* 2012, 34 (1), 93–106. [PubMed: 21845431]
7. Wu KK; Thiagarajan P, Role of endothelium in thrombosis and hemostasis. *Annu. Rev. Med* 1996, 47, 315–31. [PubMed: 8712785]
8. Mitchell JA; Ali F; Bailey L; Moreno L; Harrington LS, Role of nitric oxide and prostacyclin as vasoactive hormones released by the endothelium. *Exp. Physiol* 2008, 93 (1), 141–147. [PubMed: 17965142]

9. Packham MA; Mustard JF, Platelet aggregation and adenosine diphosphate/adenosine triphosphate receptors: A historical perspective. *Semin. Thromb. Hemost* 2005, 31 (2), 129–138. [PubMed: 15852216]
10. Deutsch M; Meinhart J; Zilla P; Howanietz N; Gorlitzer M; Froeschl A; Stuempflen A; Bezuidenhout D; Grabenwoeger M, Long-term experience in autologous in vitro endothelialization of infrainguinal ePTFE grafts. *J. Vasc. Surg* 2009, 49 (2), 352–362. [PubMed: 19110397]
11. Kumar A; Han SS, PVA-based hydrogels for tissue engineering: A review. *International Journal of Polymeric Materials and Polymeric Biomaterials* 2017, 66 (4), 159–182.
12. Chaouat M; Le Visage C; Baille WE; Escoubet B; Chaubet F; Mateescu MA; Letourneur D, A Novel Cross-linked Poly(vinyl alcohol) (PVA) for Vascular Grafts. *Adv. Funct. Mater* 2008, 18 (19), 2855–2861.
13. Cutiongco MFA; Goh SH; Aid-Launais R; Le Visage C; Low HY; Yim EKF, Planar and tubular patterning of micro and nano-topographies on poly(vinyl alcohol) hydrogel for improved endothelial cell responses. *Biomaterials* 2016, 84, 184–195. [PubMed: 26828683]
14. Cutiongco MFA; Anderson DEJ; Hinds MT; Yim EKF, In vitro and ex vivo hemocompatibility of off-the-shelf modified poly(vinyl alcohol) vascular grafts. *Acta Biomater* 2015, 25, 97–108. [PubMed: 26225735]
15. Ino JM; Sju E; Ollivier V; Yim EKF; Letourneur D; Le Visage C, Evaluation of hemocompatibility and endothelialization of hybrid poly(vinyl alcohol) (PVA)/gelatin polymer films. *J Biomed Mater Res B* 2013, 101 (8), 1549–1559.
16. Atlan M; Simon-Yarza T; Ino JM; Hunsinger V; Corte L; Ou P; Aid-Launais R; Chaouat M; Letourneur D, Design, characterization and in vivo performance of synthetic 2 mm-diameter vessel grafts made of PVA-gelatin blends. *Sci. Rep* 2018, 8. doi:10.1038/s41598-018-25703-2
17. Merkle VM; Martin D; Hutchinson M; Tran PL; Behrens A; Hossainy S; Sheriff J; Bluestein D; Wu X; Slepian MJ, Hemocompatibility of poly(vinyl alcohol)-gelatin core-shell electrospun nanofibers: A scaffold for modulating platelet deposition and activation. *ACS Applied Materials and Interfaces* 2015, 7 (15), 8302–8312. [PubMed: 25815434]
18. Tan Z; Wang H; Gao X; Liu T; Tan Y, Composite vascular grafts with high cell infiltration by co-electrospinning. *Mater. Sci. Eng., C* 2016, 67, 369–377.
19. Ruoslahti E; Pierschbacher MD, New Perspectives in Cell-Adhesion - Rgd and Integrins. *Science* 1987, 238 (4826), 491–497. [PubMed: 2821619]
20. Anderson DEJ; Truong KP; Hagen MW; Yim EKF; Hinds MT, Biomimetic Modification of Poly(vinyl alcohol): Encouraging Endothelialization and Preventing Thrombosis with Antiplatelet Monotherapy. *Acta Biomater.* 2019, 86, 291–299. [PubMed: 30639349]
21. Sekine Y; Moritani Y; Ikeda-Fukazawa T; Sasaki Y; Akiyoshi K, A Hybrid Hydrogel Biomaterial by Nanogel Engineering: Bottom-Up Design with Nanogel and Liposome Building Blocks to Develop a Multidrug Delivery System. *Advanced Healthcare Materials* 2012, 1 (6), 722–728. [PubMed: 23184823]
22. Muhammad R; Lim SH; Goh SH; Law JBK; Saifullah MSM; Ho GW; Yim EKF, Sub-100 nm patterning of TiO₂ film for the regulation of endothelial and smooth muscle cell functions. *Biomaterials Science* 2014, 2 (12), 1740–1749. [PubMed: 32481952]
23. Muhammad R; Peh GSL; Adnan K; Law JBK; Mehta JS; Yim EKF, Micro- and nano-topography to enhance proliferation and sustain functional markers of donor-derived primary human corneal endothelial cells. *Acta Biomater* 2015, 19, 138–148. [PubMed: 25796353]
24. Cutiongco MF; Anderson DE; Hinds MT; Yim EK, In vitro and ex vivo hemocompatibility of off-the-shelf modified poly(vinyl alcohol) vascular grafts. *Acta Biomater.* 2015, 25, 97–108. [PubMed: 26225735]
25. Journey PL; Anderson DEJ; Pohan G; Yim EKF; Hinds MT, Reactive Ion Plasma Modification of Poly(Vinyl-Alcohol) Increases Primary Endothelial Cell Affinity and Reduces Thrombogenicity. *Macromol. Biosci* 0 (0), 1800132.
26. Ino JM; Chevallier P; Letourneur D; Mantovani D; Le Visage C, Plasma functionalization of poly(vinyl alcohol) hydrogel for cell adhesion enhancement. *Biomater* 2013, 3 (4), e25414. [PubMed: 23989063]

27. Nuttelman CR; Mortisen DJ; Henry SM; Anseth KS, Attachment of fibronectin to poly(vinyl alcohol) hydrogels promotes NIH3T3 cell adhesion, proliferation, and migration. *J. Biomed. Mater. Res* 2001, 57 (2), 217–223. [PubMed: 11484184]
28. Tomaiuolo M; Brass LF; Stalker TJ, Regulation of Platelet Activation and Coagulation and Its Role in Vascular Injury and Arterial Thrombosis. *Interventional cardiology clinics* 2017, 6 (1), 1–12. [PubMed: 27886814]
29. Shi C; Yuan W; Khan M; Li Q; Feng Y; Yao F; Zhang W, Hydrophilic PCU scaffolds prepared by grafting PEGMA and immobilizing gelatin to enhance cell adhesion and proliferation. *Materials Science and Engineering: C* 2015, 50, 201–209. [PubMed: 25746263]
30. Rizwan M; Peh GSL; Ang HP; Lwin NC; Adnan K; Mehta JS; Tan WS; Yim EKF, Sequentially-crosslinked bioactive hydrogels as nano-patterned substrates with customizable stiffness and degradation for corneal tissue engineering applications. *Biomaterials* 2017, 120, 139–154. [PubMed: 28061402]
31. Jaipan P; Nguyen A; Narayan RJ, Gelatin-based hydrogels for biomedical applications. *Mrs Communications* 2017, 7 (3), 416–426.
32. Wang H; Feng Y; Fang Z; Xiao R; Yuan W; Khan M, Fabrication and characterization of electrospun gelatin-heparin nanofibers as vascular tissue engineering. *Macromolecular Research* 2013, 21 (8), 860–869.
33. Gorbet M; Postnikoff C; Williams S, The Noninflammatory Phenotype of Neutrophils From the Closed-Eye Environment: A Flow Cytometry Analysis of Receptor Expression. *Invest. Ophthalmol. Vis. Sci* 2015, 56 (8), 4582–4591. [PubMed: 26200498]
34. Hermanson GT, Chapter 4 - Zero-Length Crosslinkers In *Bioconjugate Techniques*(Third Edition), Hermanson GT, Ed. Academic Press: Boston, 2013; pp 259–273.
35. Chang X; Gorbet M, The effect of shear on in vitro platelet and leukocyte material-induced activation. *J. Biomater. Appl* 2013, 28 (3), 407–15. [PubMed: 22832217]
36. Italiano J EJ; Mairuhu AT; Flaumenhaft R, Clinical relevance of microparticles from platelets and megakaryocytes. *Curr. Opin. Hematol* 2010, 17 (6), 578–584. [PubMed: 20739880]
37. Sperling C; Fischer M; Maitz MF; Werner C, Blood coagulation on biomaterials requires the combination of distinct activation processes. *Biomaterials* 2009, 30 (27), 4447–56. [PubMed: 19535136]
38. Farndale RW; Sixma JJ; Barnes MJ; de Groot PG, The role of collagen in thrombosis and hemostasis. *J. Thromb. Haemost* 2004, 2 (4), 561–73. [PubMed: 15102010]
39. Lack S; Dulong V; Picton L; Cerf DL; Condamine E, High-resolution nuclear magnetic resonance spectroscopy studies of polysaccharides crosslinked by sodium trimetaphosphate: a proposal for the reaction mechanism. *Carbohydr. Res* 2007, 342 (7), 943–953. [PubMed: 17303095]
40. Macrí-Pellizzeri L; Pelacho B; Sancho A; Iglesias-García O; Simón-Yarza AM; Soriano-Navarro M; González-Granero S; García-Verdugo JM; De-Juan-Pardo EM; Prosper F, Substrate stiffness and composition specifically direct differentiation of induced pluripotent stem cells. *Tissue Engineering - Part A* 2015, 21 (9–10), 1633–1641. [PubMed: 25668195]
41. Hassan CM; Peppas NA, Structure and Morphology of Freeze/Thawed PVA Hydrogels. *Macromolecules* 2000, 33 (7), 2472–2479.
42. Cutiongco MFA; Kukumberg M; Peneyra JL; Yeo MS; Yao JY; Rufaihah AJ; Le Visage C; Ho JP; Yim EKF, Submillimeter Diameter Poly(Vinyl Alcohol) Vascular Graft Patency in Rabbit Model. *Frontiers in Bioengineering and Biotechnology* 2016, 4 (44). 10.3389/fbioe.2016.00044
43. Alexandre N; Ribeiro J; Gärtner A; Pereira T; Amorim I; Fragoso J; Lopes A; Fernandes J; Costa E; Santos-Silva A; Rodrigues M; Santos JD; Maurício AC; Luís AL, Biocompatibility and hemocompatibility of polyvinyl alcohol hydrogel used for vascular grafting - In vitro and in vivo studies. *Journal of Biomedical Materials Research - Part A* 2014, 102 (12), 4262–4275. [PubMed: 24488670]
44. Alexandre N; Amorim I; Caseiro AR; Pereira T; Alvites R; Rêma A; Gonçalves A; Valadares G; Costa E; Santos-Silva A; Rodrigues M; Lopes MA; Almeida A; Santos JD; Maurício AC; Luís AL, Long term performance evaluation of small-diameter vascular grafts based on polyvinyl alcohol hydrogel and dextran and MSCs-based therapies using the ovine pre-clinical animal model. *Int. J. Pharm* 2017, 523 (2), 515–530. [PubMed: 28283218]

45. Lin JH; Hu JJ; Tu CY; Lee MC; Lu CT; Lu PC; Chen YS; Lou CW, Tubular polyvinyl alcohol composites used as vascular grafts: Manufacturing techniques and property evaluations. *Mater. Lett* 2017, 190, 201–204.
46. Alexandre N; Costa E; Coimbra S; Silva A; Lopes A; Rodrigues M; Santos M; Maurício AC; Santos JD; Luís AL, In vitro and in vivo evaluation of blood coagulation activation of polyvinyl alcohol hydrogel plus dextran-based vascular grafts. *Journal of Biomedical Materials Research - Part A* 2015, 103 (4), 1366–1379. [PubMed: 25044790]
47. Rafat M; Rotenstein LS; You J-O; Auguste DT, Dual functionalized PVA hydrogels that adhere endothelial cells synergistically. *Biomaterials* 2012, 33 (15), 3880–3886. [PubMed: 22364701]
48. Gallant ND; Michael KE; García AJ, Cell Adhesion Strengthening: Contributions of Adhesive Area, Integrin Binding, and Focal Adhesion Assembly. *Mol. Biol. Cell* 2005, 16 (9), 4329–4340. [PubMed: 16000373]
49. Kim D-H; Wirtz D, Predicting how cells spread and migrate. *Cell Adhesion & Migration* 2013, 7 (3), 293–296. [PubMed: 23628962]
50. Tee S-Y; Fu J; Chen, Christopher S.; Janmey, Paul A., Cell Shape and Substrate Rigidity Both Regulate Cell Stiffness. *Biophys. J* 2011, 100 (5), L25–L27. [PubMed: 21354386]
51. Yim EKF; Sheetz MP, Force-dependent cell signaling in stem cell differentiation. *Stem Cell Res Ther* 2012, 3. doi:10.1186/scrt132 [PubMed: 22277374]
52. Attwood SJ; Cortes E; Haining AWM; Robinson B; Li D; Gautrot J; del Río Hernández A, Adhesive ligand tether length affects the size and length of focal adhesions and influences cell spreading and attachment. *Sci. Rep* 2016, 6, 34334. [PubMed: 27686622]
53. Cavalcanti-Adam EA; Volberg T; Micoulet A; Kessler H; Geiger B; Spatz JP, Cell Spreading and Focal Adhesion Dynamics Are Regulated by Spacing of Integrin Ligands. *Biophysical Journal* 2007, 92 (8), 2964–2974. [PubMed: 17277192]
54. Davies PF, Hemodynamic shear stress and the endothelium in cardiovascular pathophysiology. *Nat Clin Pract Cardiovasc Med* 2009, 6 (1), 16–26. [PubMed: 19029993]
55. Reglero-Real N; Colom B; Bodkin JV; Nourshargh S, Endothelial Cell Junctional Adhesion Molecules: Role and Regulation of Expression in Inflammation. *Arterioscler. Thromb. Vasc. Biol* 2016, 36 (10), 2048–2057. [PubMed: 27515379]
56. Zhang X; Thomas V; Xu Y; Bellis SL; Vohra YK, An in vitro regenerated functional human endothelium on a nanofibrous electrospun scaffold. *Biomaterials* 2010, 31 (15), 4376–4381. [PubMed: 20199808]
57. Harrington WF; Von Hippel PH, The Structure Of Collagen And Gelatin In *Adv. Protein Chem*, Anfinsen CB; Anson ML; Bailey K; Edsall JT, Eds. Academic Press: 1962; Vol. 16, pp 1–138.
58. Inoue O; Suzuki-Inoue K; Dean WL; Frampton J; Watson SP, Integrin $\alpha 2\beta 1$ mediates outside-in regulation of platelet spreading on collagen through activation of Src kinases and PLC $\gamma 2$. *The Journal of Cell Biology* 2003, 160 (5), 769–780. [PubMed: 12615912]
59. Giol ED; Van Vlierberghe S; Unger RE; Schaubroeck D; Ottevaere H; Thienpont H; Kirkpatrick CJ; Dubruel P, Endothelialization and Anticoagulation Potential of Surface-Modified PET Intended for Vascular Applications. *Macromol. Biosci* 2018, 18 (7), 1800125.
60. Xiong GM; Yuan S; Tan CK; Wang JK; Liu Y; Yang Tan TT; Tan NS; Choong C, Endothelial cell thrombogenicity is reduced by ATRP-mediated grafting of gelatin onto PCL surfaces. *Journal of Materials Chemistry B* 2014, 2 (5), 485–493. [PubMed: 32261529]
61. Han F; Jia X; Dai D; Yang X; Zhao J; Zhao Y; Fan Y; Yuan X, Performance of a multilayered small-diameter vascular scaffold dual-loaded with VEGF and PDGF. *Biomaterials* 2013, 34 (30), 7302–7313. [PubMed: 23830580]
62. Kar K; Amin P; Bryan MA; Persikov AV; Mohs A; Wang YH; Brodsky B, Self-association of collagen triple helix peptides into higher order structures. *J. Biol. Chem* 2006, 281 (44), 33283–90. [PubMed: 16963782]

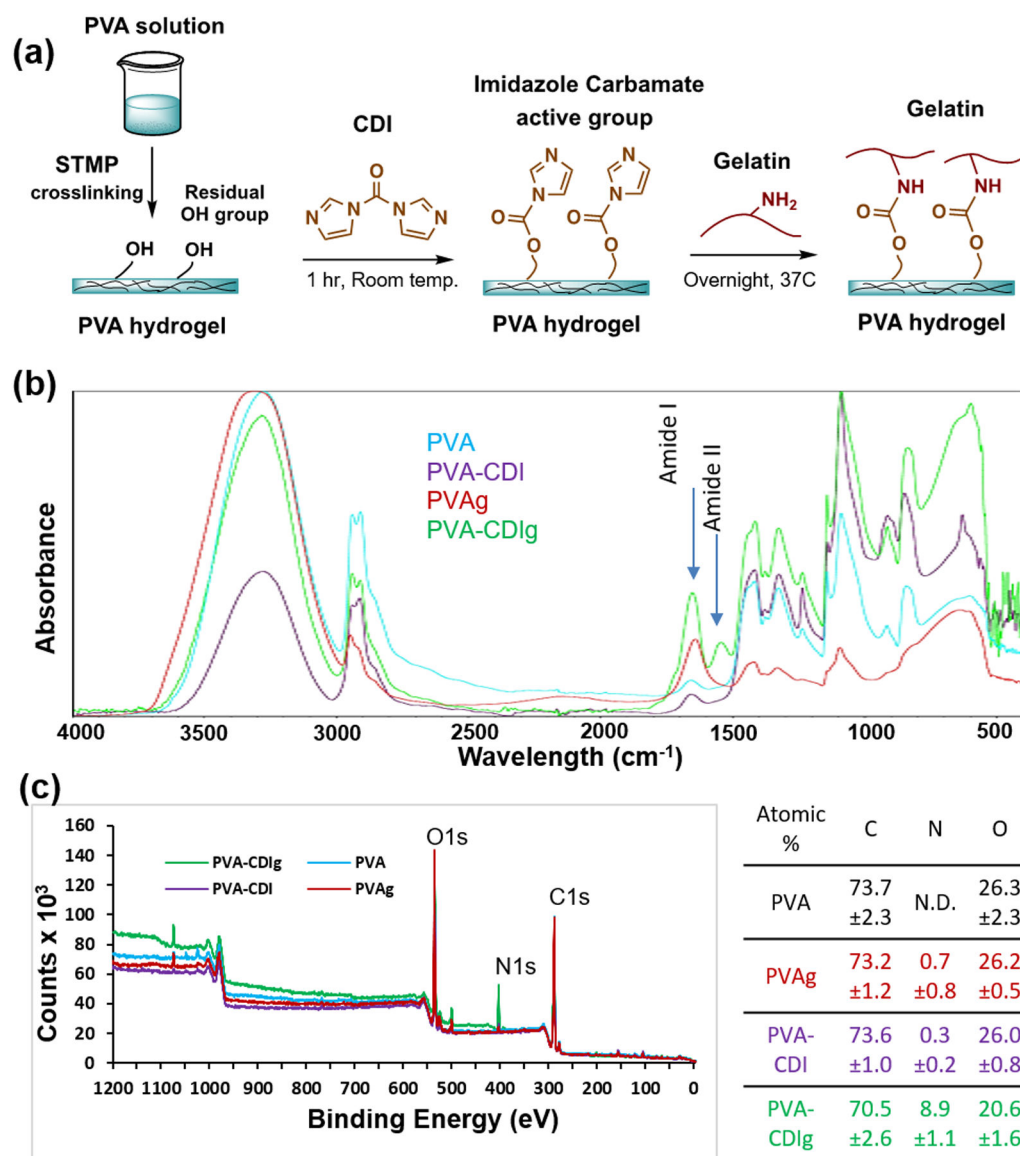


Figure 1:

(a) Schematic diagram of the reaction to conjugate gelatin onto PVA via hydroxyl-to-amine coupling. Carbonyldiimidazole (CDI) was used to activate the hydroxyl groups on the PVA (b) Fourier-transform infrared spectroscopy (FTIR) graph showing the Amide I and Amide II peaks in the gelatin-conjugated PVA (PVA-CDIg). (c) X-ray photoelectron spectroscopy (XPS) survey scan of PVA, PVA-CDI and PVA-CDIg. The table shows the atomic %age of carbon, nitrogen and oxygen and SD (n=3). N.D. = Not determined

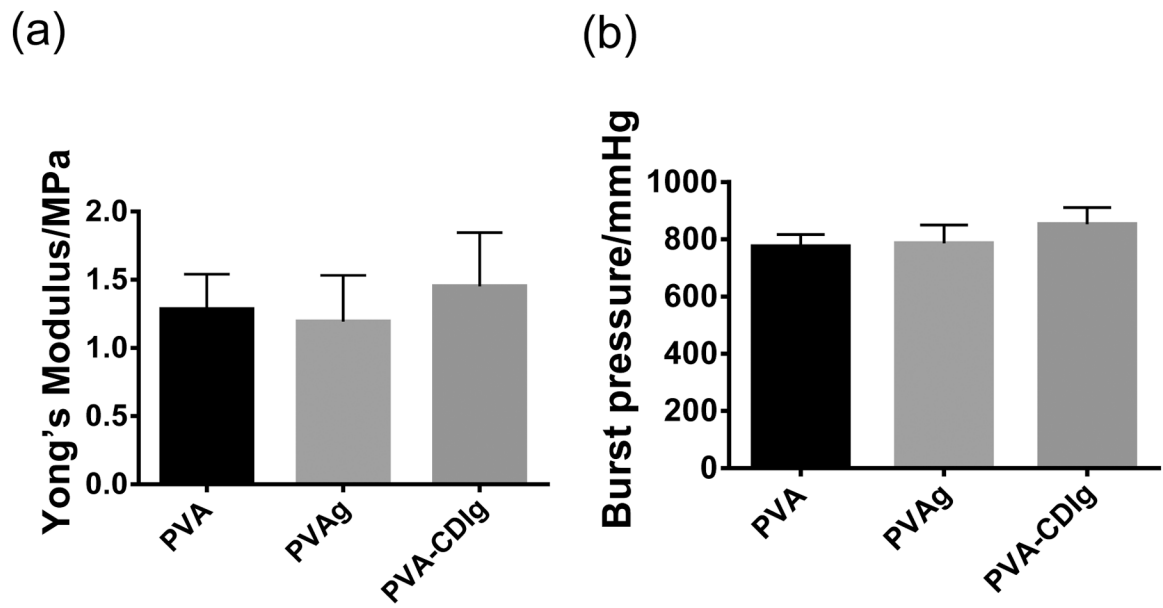


Figure 2:
Effect of gelatin conjugation on the (a) burst pressure and (b) tensile Young's modulus of the PVA, PVAg, and PVA-CDIg. n=3. Data are not statistically significant different.

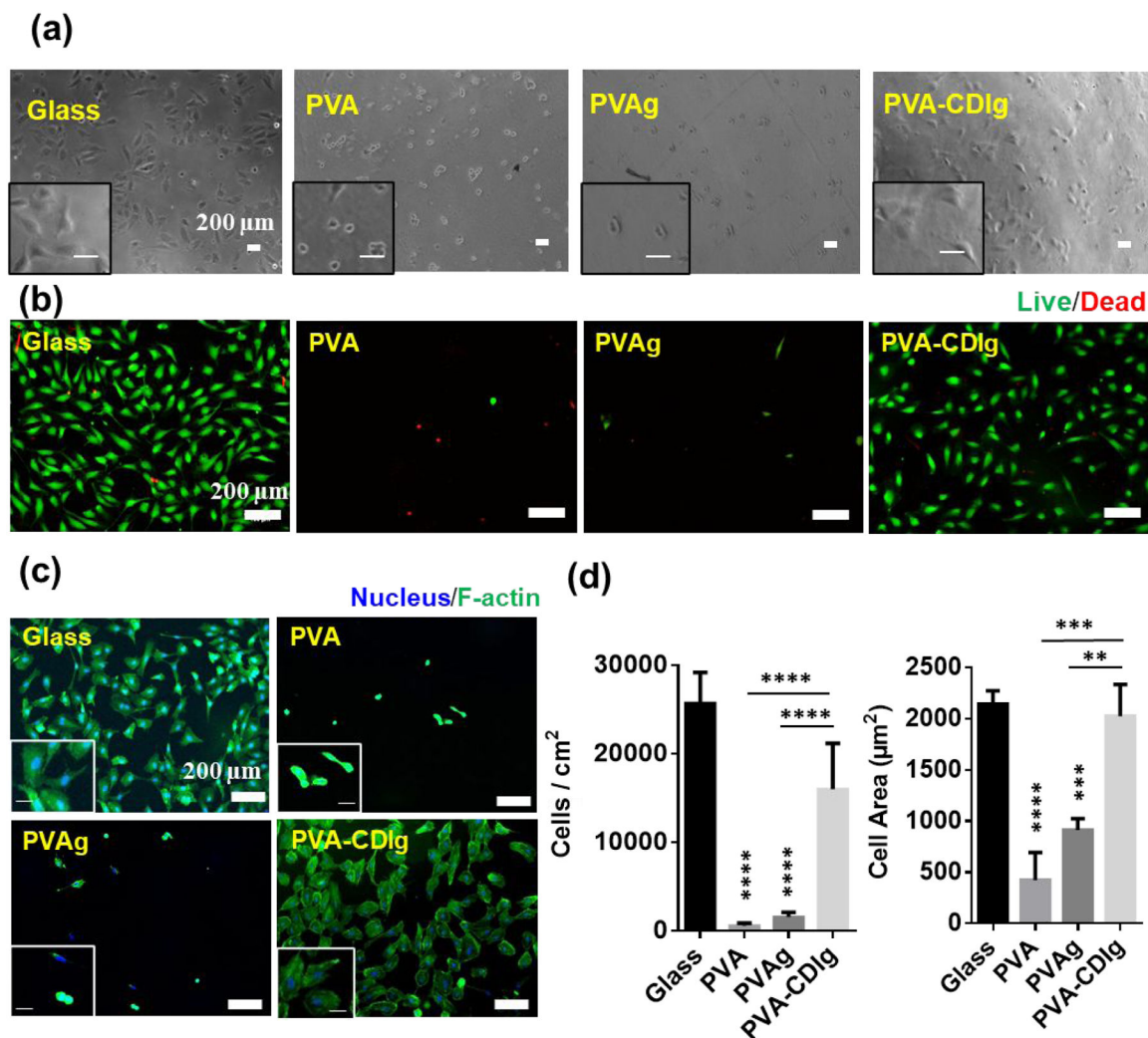
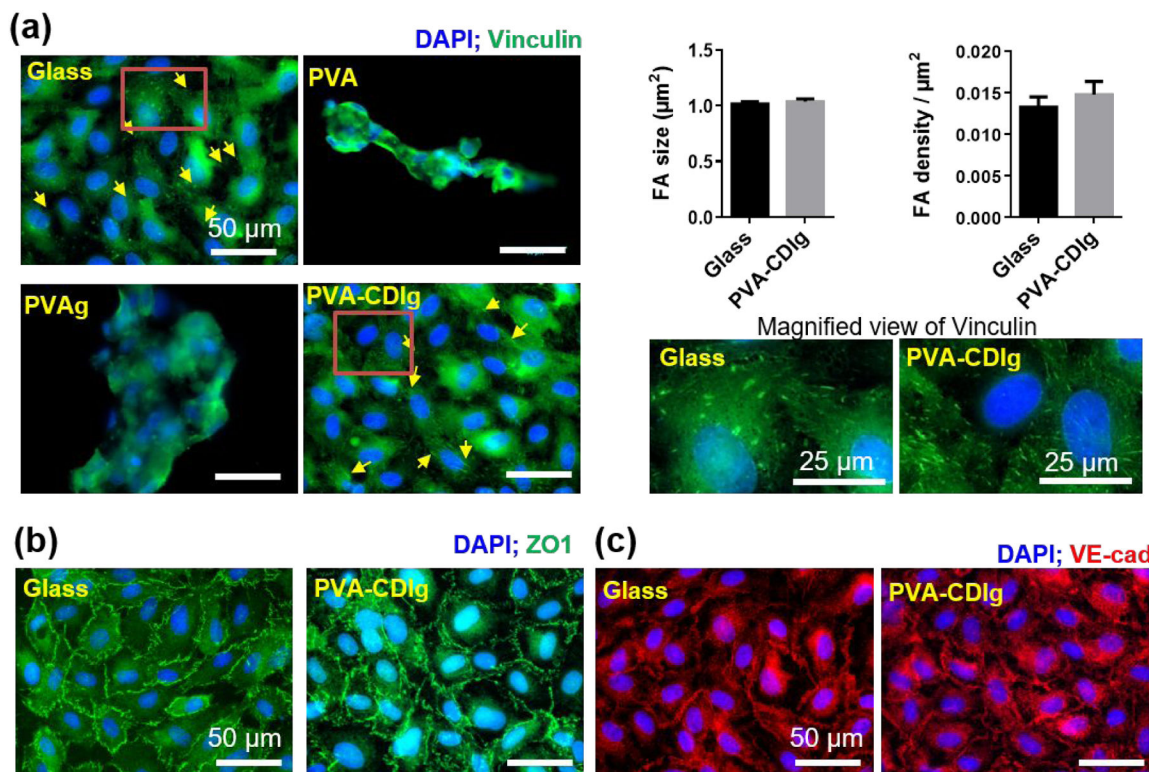


Figure 3:

(a) Phase contrast images showing the attachment of primary Human umbilical vein endothelial cells (HUVEC) attachment after 4 hrs of seeding on glass, unmodified PVA, PVA incubated in gelatin (PVAg) and gelatin-grafted PVA (PVA-CDIg). Inset shows magnified view. (Scale bar=200 μm) (b) Results of the live-dead assay on glass, PVA, PVAg and PVA-CDIg to assess the viability of the cells after 24 hrs of seeding. Dead cells are stained red. (Scale bar=200 μm) (c) Cell spreading was analyzed by phalloidin staining of the cell (green). Inset shows magnified view. (Scale bar=200 μm) (d) Quantification of the cell area and density by using phalloidin stained image analysis in ImageJ. * represent statistical significance compared to glass control. Statistical significance between different groups (if any) is shown by connecting lines. * $P < 0.05$, ** $P < 0.01$, *** $P < 0.001$, **** $P < 0.0001$ (n = 3, ANOVA, Tukey post-hoc)

**Figure 4:**

(a) Focal adhesion (FAs) expression as investigated by vinculin staining (green). HUVECs on gelatin-grafted PVA (PVA-CDIg) expressed focal adhesions, which were comparable to HUVECs on glass controls. HUVECs grown on unmodified PVA or PVAg did not express focal adhesions. Panel on the right display magnified view of vinculin FAs on glass and PVA-CDIg. Bar graphs on the right display semi-quantitative analysis of FA size and density on glass vs PVA-CDIg, which were comparable ($n = 3$). (b) Tight junctional protein zonula occludens 1 (ZO1) expression on glass and PVA-CDIg. HUVECs on unmodified PVA and PVAg were not analyzed because cell attachment was poor. (c) VE-cadherin (VE-Cad) expression on glass and PVA-CDIg. HUVECs on unmodified PVA and PVAg were not analyzed because cell attachment was poor.

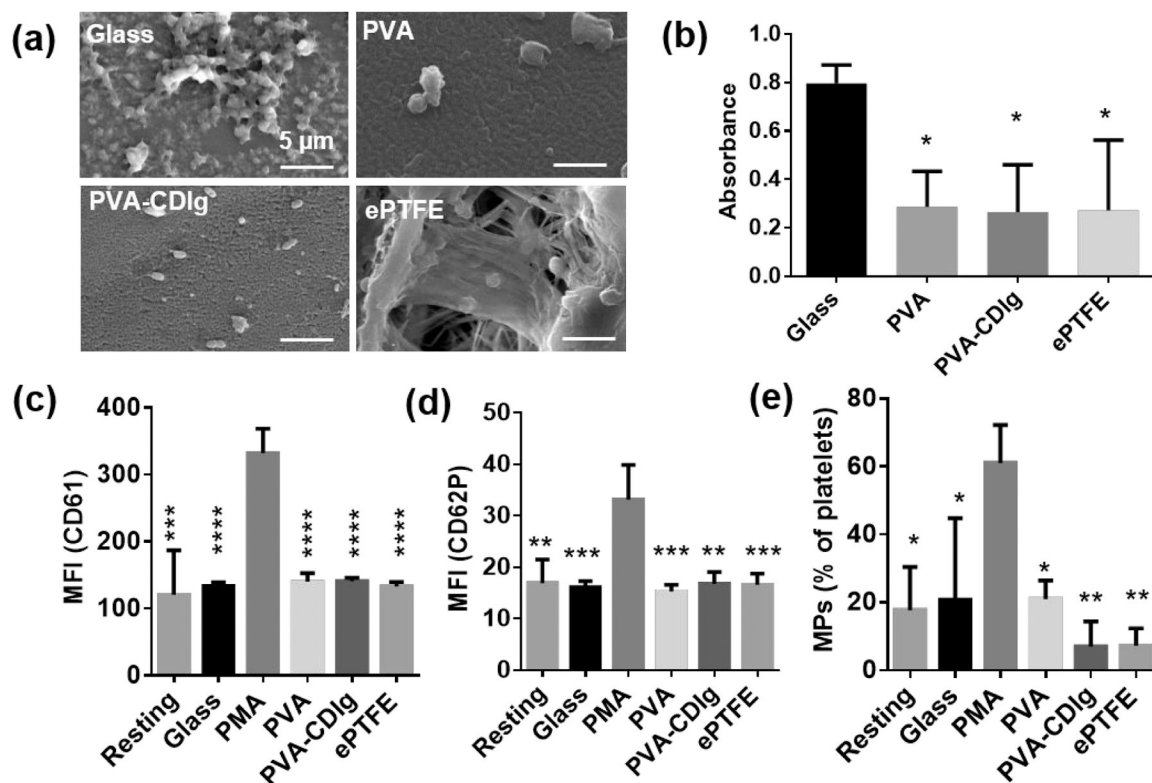


Figure 5:

(a) SEM images of platelet adhesion and morphology on ePTFE (clinical control), collagen coated glass (positive control), PVA and PVA-CDIlg. Platelets adhesion on PVA-CDIlg was comparable to PVA and ePTFE. (b) Lactate dehydrogenase (LDH) assay for relative quantification of platelets adhesion on different materials. Absorbance in LDH assay correlates with the platelet adhesion. Flow cytometry analysis of the platelets activation in suspension in terms of (c) Mean fluorescence intensity (MFI) of CD61 (also known as integrin $\beta 3$ or glycoprotein IIIa) (d) Mean fluorescence intensity (MFI) of CD62p (P-selectin) and (e) Microparticles (MPs) generated as percentage of CD61+ platelets. * represent statistical significance compared to glass control (LDH assay) or compared to PMA control (Flow cytometry data). * $P < 0.05$, ** $P < 0.01$, *** $P < 0.001$, **** $P < 0.0001$ (n = 3)

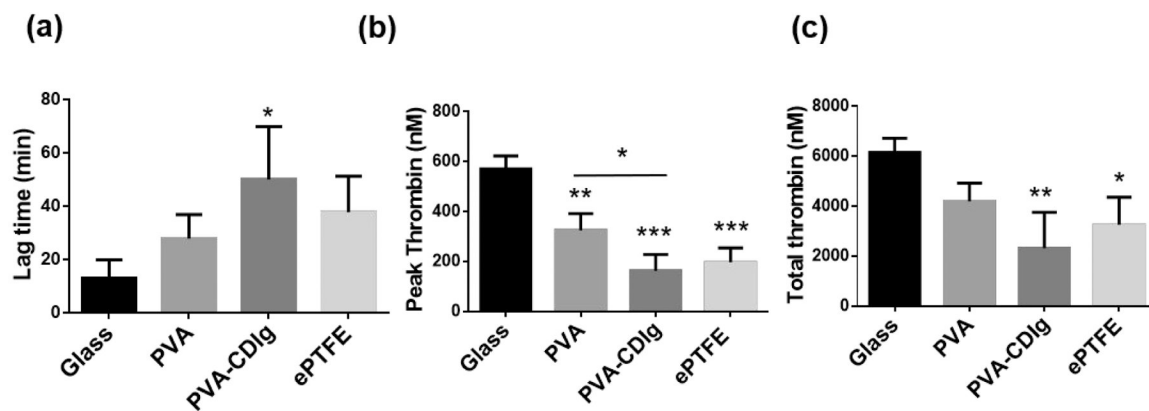


Figure 6:

Results of the fluorescence measurement based real time thrombin formation assay. Human donor platelet rich plasma collected after incubation with different samples for 1 hr was used to analyze the thrombin formation. (a) Lagtime, which represents time taken before the thrombin generation can be observed after the assay is started. Higher lagtime shows a lower tendency of blood plasma to form thrombus (b) Peak thrombin formation, which was significantly lower on PVA-CDIg compared to PVA (c) Total thrombin formed during the assay. * represent statistical significance compared to glass control. Statistical significance between different groups (if any) is shown by connecting lines. *P < 0.05, **P < 0.01, ***P < 0.001, ****P < 0.0001 (n = 3, ANOVA, Tukey post hoc)

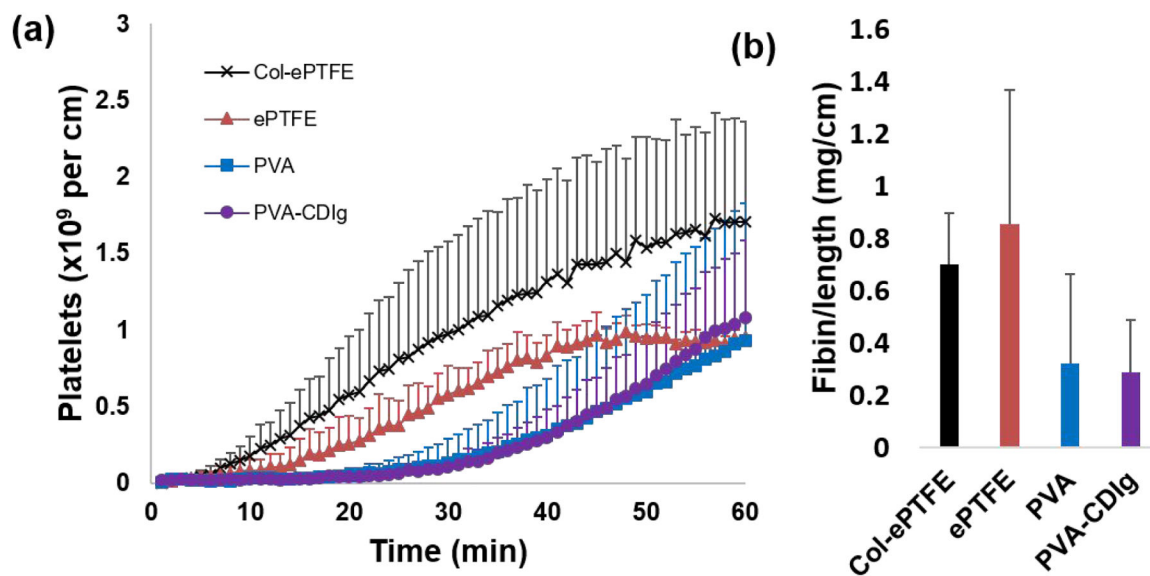


Figure 7: PVA-CDIg, plain PVA, ePTFE, and collagen-coated ePTFE tubes were tested in a chronic, *ex vivo* shunt model in a well-established non-human primate model. (a) Platelet accumulation was measured dynamically for 1hr. (b) Fibrin accumulation was tested and normalized per cm of graft length and showed no significant differences between any of the groups. Fibrin accumulation on PVA-CDIg and PVA was comparable (n = 2–6).